

# Forward $K^+$ -production in subthreshold $pA$ collisions at 1.0 GeV

V. Koptev,<sup>1</sup> M. Büscher,<sup>2</sup> H. Junghans,<sup>2</sup> M. Nikipelov,<sup>1,2</sup> K. Sistemich,<sup>2</sup> H. Ströher,<sup>2</sup> V. Abaev,<sup>1</sup> H.-H. Adam,<sup>3</sup> R. Baldauf,<sup>4</sup> S. Barsov,<sup>1</sup> U. Bechstedt,<sup>2</sup> N. Bongers,<sup>2</sup> G. Borchert,<sup>2</sup> W. Borgs,<sup>2</sup> W. Bräutigam,<sup>2</sup> W. Cassing,<sup>5</sup> V. Chernyshev,<sup>6</sup> B. Chiladze,<sup>7</sup> M. Debowski,<sup>8</sup> J. Dietrich,<sup>2</sup> M. Drochner,<sup>4</sup> S. Dymov,<sup>9</sup> J. Ernst,<sup>10</sup> W. Erven,<sup>4</sup> R. Esser,<sup>11\*</sup> P. Fedorets,<sup>6</sup> A. Franzen,<sup>2</sup> D. Gotta,<sup>2</sup> T. Grande,<sup>2</sup> D. Grzonka,<sup>2</sup> G. Hansen,<sup>12</sup> M. Hartmann,<sup>2</sup> V. Hejny,<sup>2</sup> L.v. Horn,<sup>2</sup> L. Jarczyk,<sup>13</sup> A. Kacharava,<sup>9</sup> B. Kamys,<sup>13</sup> A. Khoukaz,<sup>3</sup> T. Kirchner,<sup>8</sup> S. Kistryn,<sup>13</sup> F. Klehr,<sup>12</sup> H.R. Koch,<sup>2</sup> V. Komarov,<sup>9</sup> S. Kopyto,<sup>2</sup> R.Krause,<sup>2</sup> P. Kravtsov,<sup>1</sup> V. Kruglov,<sup>9</sup> P. Kulesa,<sup>2,13</sup> A. Kulikov,<sup>9,14</sup> V. Kurbatov,<sup>9</sup> N. Lang,<sup>3</sup> N. Langenhagen,<sup>8</sup> I. Lehmann,<sup>2</sup> A. Leppes,<sup>2</sup> J. Ley,<sup>11</sup> B. Lorentz,<sup>2</sup> G. Macharashvili,<sup>7,9</sup> R. Maier,<sup>2</sup> S. Martin,<sup>2</sup> S. Merzliakov,<sup>9</sup> K. Meyer,<sup>2</sup> S. Mikirtychiants,<sup>1</sup> H. Müller,<sup>8</sup> P. Munhofen,<sup>2</sup> A. Mussgiller,<sup>2</sup> V. Nelyubin,<sup>1</sup> M. Nioradze,<sup>7</sup> H. Ohm,<sup>2</sup> A. Petrus,<sup>9</sup> D. Prasuhn,<sup>2</sup> B. Prietzsch,<sup>8</sup> H.J. Probst,<sup>2</sup> D. Protic,<sup>2</sup> K. Pysz,<sup>15</sup> F. Rathmann,<sup>2</sup> B. Rimarzig,<sup>8</sup> Z. Rudy,<sup>13</sup> R. Santo,<sup>3</sup> H. Paetz gen. Schieck,<sup>11</sup> R. Schleichert,<sup>2</sup> A. Schneider,<sup>2</sup> Chr. Schneider,<sup>8</sup> H. Schneider,<sup>2</sup> G. Schug,<sup>2</sup> O.W.B. Schult,<sup>2</sup> H. Seyfarth,<sup>2</sup> A. Sibirtsev,<sup>2</sup> J. Smyrski,<sup>13</sup> H. Stechemesser,<sup>12</sup> E. Steffens,<sup>16</sup> H.J. Stein,<sup>2</sup> A. Strzalkowski,<sup>13</sup> K.-H. Watzlawik,<sup>2</sup> C. Wilkin,<sup>17</sup> P. Wüstner,<sup>4</sup> S. Yashenko,<sup>9</sup> B. Zalikhanov,<sup>9</sup> N. Zhuravlev,<sup>9</sup> P. Zolnierczuk,<sup>13</sup> K. Zwill,<sup>4</sup> I. Zychor,<sup>18</sup>

<sup>1</sup>High Energy Physics Department, Petersburg Nuclear Physics Institute, 188350 Gatchina, Russia

<sup>2</sup>Institut für Kernphysik, Forschungszentrum Jülich, 52425 Jülich, Germany

<sup>3</sup>Institut für Kernphysik, Universität Münster, W.-Klemm-Str. 9, D-48149 Münster, Germany

<sup>4</sup>Zentralinstitut für Elektronik, Forschungszentrum Jülich, 52425 Jülich, Germany

<sup>5</sup>Institut für Theoretische Physik, Universität Gießen, H.-Buff-Ring 16, D-35392 Gießen, Germany

<sup>6</sup>Institute for Theoretical and Experimental Physics, Cheremushkinskaya 25, 117259 Moscow, Russia

<sup>7</sup>High Energy Physics Institute, Tbilisi State University, University Street 9, 380086 Tbilisi, Georgia

<sup>8</sup>Institut für Kern- und Hadronenphysik, Forschungszentrum Rossendorf, D-01474 Dresden, Germany

<sup>9</sup>Laboratory of Nuclear Problems, Joint Institute for Nuclear Research, 141980 Dubna, Russia

<sup>10</sup>Institut für Strahlen- und Kernphysik, Universität Bonn, Nußallee 14, D-53115 Bonn, Germany

<sup>11</sup>Institut für Kernphysik, Universität zu Köln, Zùlpicher Str. 77, 50937 Köln, Germany

<sup>12</sup>Zentralabteilung Technologie, Forschungszentrum Jülich, 52425 Jülich, Germany

<sup>13</sup>Institute of Physics, Jagellonian University, Reymonta 4, 30059 Cracow, Poland

<sup>14</sup>Dubna Branch, Moscow State University, 141980 Dubna Moscow Region, Russia

<sup>15</sup>Institute of Nuclear Physics, Radzikowskiego 152, PL-31342, Cracow, Poland

<sup>16</sup>Physikalisches Institut II, Universität Erlangen-Nürnberg, Erwin-Rommel-Str. 1, D-91058 Erlangen, Germany

<sup>17</sup>Physics Department, UCL, Gower Street, London WC1 6BT, England

<sup>18</sup>The Andrzej Soltan Institute for Nuclear Studies, 05400 Swierk, Poland

(October 24, 2018)

$K^+$ -meson production in  $pA$  ( $A = C, Cu, Au$ ) collisions has been studied using the ANKE spectrometer at an internal target position of the COSY-Jülich accelerator. The complete momentum spectrum of kaons emitted at forward angles,  $\vartheta \leq 12^\circ$ , has been measured for a beam energy of  $T_p = 1.0$  GeV, far below the free  $NN$  threshold of 1.58 GeV. The spectrum does not follow a thermal distribution at low kaon momenta and the larger momenta reflect a high degree of collectivity in the target nucleus.

A central topic of hadron physics is the influence of the nuclear medium on elementary processes. This question can be studied by measuring the production of mesons in nuclei using projectiles with energies below the threshold for free  $NN$  collisions (so-called subthreshold production). These processes necessarily involve cooperative effects of the nucleons inside the target nucleus. The investigation of  $K^+$ -production is particularly well suited for this purpose since the meson is relatively heavy so that

its production requires strong medium effects. Furthermore, the  $K^+$  scatters little in nuclear matter so that its final-state interactions are expected to be small.

Proton-induced  $K^+$ -production at subthreshold energies has been studied at several accelerators. Total cross sections have been measured at the PNPI synchrotron for targets between Be and Pb and projectile energies  $T_p$  from 0.8 to 1.0 GeV [1]. The results were discussed in terms of different models [1–5], in particular of single or two-step reactions involving the creation of an intermediate pion. It was concluded that additional experimental data were needed for an unambiguous determination of the reaction mechanism and the extraction of the information on nuclear-medium effects. Inclusive differential cross sections for  $pA$ -interactions have been studied at BEVALAC [6], SATURNE [7] and CELSIUS [8]. Partial momentum spectra have been obtained at laboratory emission angles of  $10^\circ, 15^\circ, 35^\circ, 40^\circ, 60^\circ, 80^\circ$  and  $90^\circ$ , at projectile energies down to 1.2 GeV and evidence for the dominance of the two-step processes has been observed at the lowest  $T_p$ . Subthreshold production has also been studied at the ITEP-synchrotron [9],

where kaons with high momenta were identified at projectile proton energies of 1.75 to 2.6 GeV, and in heavy-ion reactions at GANIL [10] and GSI [11].

The COoler SYNchrotron COSY-Jülich [12], which provides proton beams in the range  $T_p = 0.04 - 2.65$  GeV, is well suited for the study of  $K^+$ -production. In measurements with very thin windowless internal targets, secondary processes of the produced mesons can be neglected. Subthreshold  $K^+$ -production was a prime motivation for building the ANKE spectrometer [13,14] within one straight section of the COSY ring. It consists of three dipole magnets D1–D3, see Fig. 1, which separate forward-emitted reaction products from the circulating proton beam and allow a determination of their emission angles and momenta. The layout of the device, including detectors and the data-acquisition (DAQ) system, was optimized for the study of  $K^+$ -spectra down to  $T_p = 1.0$  GeV. This is a very demanding task because of the small  $K^+$ -production cross sections, e.g. 39 nb for  $pC$  collisions at 1.0 GeV [1]. Kaons have to be identified in a background of secondary protons and pions which is up to  $10^6$  times more intense.  $K^+$ -identification is described in detail in [15,16]; only basic features of the procedures are summarized here.

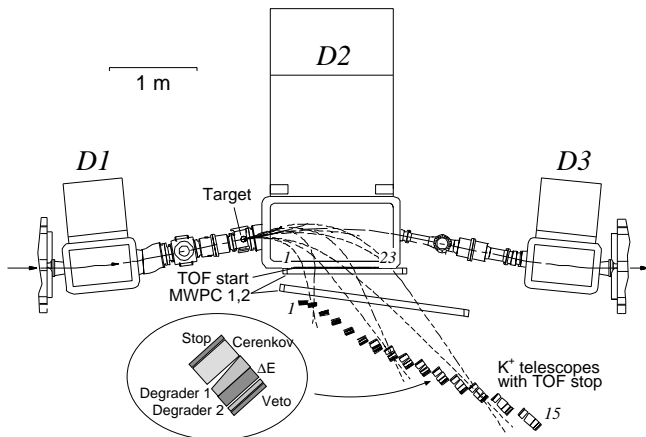


FIG. 1. Top view of the ANKE spectrometer in the COSY ring and detectors used for  $K^+$  identification. The inset shows the components of one of the range telescopes. Typical kaon trajectories are indicated. Details can be found in [13–16].

The COSY ring was filled with  $2 - 4 \times 10^{10}$  protons per cycle and cycle times were typically 30 s. The protons were accelerated to 1.0 GeV on an orbit below the target and then raised by steerers such that the rate in the ANKE detectors was kept constant and on a level that could be handled by the DAQ system. Thin strip targets of C (polycrystalline diamond), Cu and Au with thicknesses of 40–1500  $\mu\text{g}/\text{cm}^2$  were used. Reaction products were detected with an array of 15 range telescopes positioned along the focal surface. The time-of-flight (TOF) was measured with 0.5 to 2 mm thick start scintillators (23 detectors of 5 cm width) and 1 cm thick (10 cm wide) stop scintillators which are components of the telescopes, see Fig. 1. Due to the momentum focussing of the dipole

D2, the telescopes can be used to identify different ejectiles via their ranges: protons are stopped before reaching the  $\Delta E$  counters,  $K^+$ -mesons come to rest before the veto counters, while pions give signals in all detectors. Copper degraders are used to slow down the kaons in front of the  $\Delta E$  counters (degrader 1) and prevent them from reaching the veto counters (degrader 2). Pions and muons from the decay of stopped kaons are emitted isotropically, and partially detected in the veto counter, with a characteristic delay corresponding to the kaon lifetime  $\tau = 12.4$  ns. The multiwire proportional chambers MWPC 1 and 2 allow one to determine the ejectile tracks and hence separate particles originating from the target from scattered background, e.g., from the pole shoes of D2. Applying the criteria *i*) TOF, *ii*) energy losses in the scintillation counters, *iii*) delayed signals in the veto counters and *iv*) track origin in the target, it is possible to identify unambiguously  $K^+$ -mesons [15]. Criteria *i*) and *iii*) were applied on-line to decrease the amount of data written to tape.

The typical number of identified  $K^+$ -mesons,  $N_{\text{tel}(i)}^K$ , in one telescope *i* during a four days run on *C* was 100. Since each telescope covers a given momentum range, the  $N_{\text{tel}(i)}^K$  determine directly the momentum distribution. The accepted momentum bites range from 13% at the low momentum side of the telescope array ( $\sim 150$  MeV/c) to 7% for high momenta ( $\sim 510$  MeV/c). The vertical angular acceptance of ANKE varies between  $\vartheta_V = \pm 7^\circ$  and  $\pm 3.5^\circ$  for the low- and high-momentum telescopes, respectively. In the horizontal direction, ejectiles with emission angles  $|\vartheta_H| \leq 12^\circ$  were accepted by the on-line TOF-trigger system [15].

Double differential cross sections for  $K^+$ -production were obtained from  $N_{\text{tel}(i)}^K$  by comparison with the number of pions  $N_{\text{stop}(i)}^\pi$  detected in the stop counters of the same telescope, which were measured in dedicated calibration runs. The ratio of  $K^+$  and  $\pi^+$  counts was corrected for the different detection efficiencies  $\epsilon$  and normalized to the corresponding proton-beam fluxes  $M^\pi$  and  $M^K$  (i.e. luminosities) and to the cross sections of  $\pi^+$  production in  $pC$  interactions in the forward direction at 1.0 GeV [17–19]. Due to their much larger production cross section, pions can be identified applying only criteria *i*) and *iv*). The cross section is thus given by:

$$\frac{d^2\sigma^K}{d\Omega dp} = \frac{d^2\sigma^\pi}{d\Omega dp} \cdot \frac{N_{\text{tel}(i)}^K}{N_{\text{stop}(i)}^\pi} \cdot \frac{M^\pi}{M^K} \cdot \frac{1}{\epsilon} \quad (1)$$

$$\epsilon = \frac{\epsilon_{\text{tel}(i)}^K \cdot \epsilon_{\text{MWPC}(i)}^K \cdot \epsilon_{\text{decay}}^K}{\epsilon_{\text{stop}(i)}^\pi \cdot \epsilon_{\text{MWPC}(i)}^\pi \cdot \epsilon_{\text{decay}}^\pi},$$

where  $\epsilon_{\text{tel}(i)}^K$  is the  $K^+$ -identification efficiency of the *i*<sup>th</sup> telescope including the detection probability for the decay muons and pions. Only events where veto counter signals were delayed by at least 2.5 ns with respect to those of the stopped kaons were considered. The efficiencies,  $\epsilon_{\text{tel}(i)}^K \sim 0.1 - 0.3$ , were obtained from a calibration

run at  $T_p = 2.3$  GeV, where  $K^+$ -production is significantly larger [15].

The average pion detection efficiencies  $\epsilon_{\text{stop}(i)}^\pi = 0.98$ . The MWPC efficiencies  $\epsilon_{\text{MWPC}}$  are in the range 0.97–0.99 both for pions and kaons.  $\epsilon_{\text{decay}}^K$  and  $\epsilon_{\text{decay}}^\pi$  take into account losses in flight between target and stop counters; they were determined by simulations as 0.30–0.36 for kaons and 0.85–0.88 for pions. Relative monitoring of the proton beam interacting with the target nuclei  $A$  ( $M_A^K$  and  $M_A^\pi$ ) was done with an accuracy of 2% using 4-fold coincidences of telescopes 2, 3, 4 and 5 (selection of ejectiles by-passing the spectrometer dipole D2).

Our double differential cross section for  $K^+$  production in proton-carbon interactions at  $T = 1.0$  GeV is shown in Fig. 2a). In contrast to measurements at higher energies [6–9,20], ANKE reveals, for the first time, a complete momentum spectrum at deep subthreshold energies.

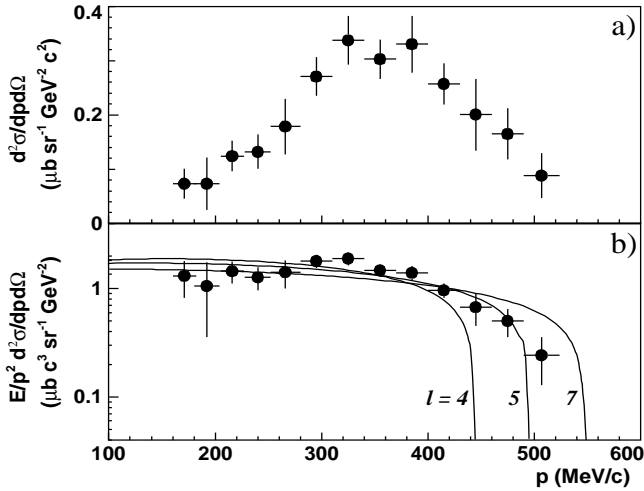


FIG. 2. a) Double differential  $K^+$ -production cross section for the  $p(1.0 \text{ GeV})^{12}\text{C} \rightarrow K^+(\vartheta \leq 12^\circ)X$  reaction as a function of the  $K^+$ -momentum. b) Same data plotted as invariant cross section. The error bars are purely statistical. The overall normalization uncertainty is estimated to be 10%. The solid lines describe the behavior of the invariant cross section within a phase-space approximation (Eq. (2)).

The *low-momentum* part of the  $K^+$ -spectrum in Fig. 2b) cannot be described by a thermal distribution,  $E/p^2 d^2\sigma/dp d\Omega \propto \exp(-T^*/T_0)$ , where  $T^*$  is the  $K^+$  kinetic energy in the beam-proton nucleus system. Such distributions had been assumed to deduce total cross sections from earlier measurements with limited momentum intervals [6–8,20].

A high degree of collectivity is needed in the target nucleus to allow  $K^+$ -production far below the free NN-threshold, i.e. the number of target nucleons involved must be significantly larger than one [1–5]. Alternatively, high intrinsic momenta of the participating target nucleon(s) are required to supply the missing energy for subthreshold kaon production. This is particularly the case for the *high-momentum* part of the kaon spectrum: internal momenta of a single nucleon of at least

$p_N \sim 350(550)$  MeV/c would be needed in order to produce kaons in the forward direction with momenta of  $p_K \sim 260(500)$  MeV/c. High momentum components above  $\sim 500$  MeV/c are essentially due to many-body correlations in the nucleus [21].

To get a rough estimate of the number of participating nucleons, we describe the invariant cross section within a phase-space approximation. This method has previously been applied to  $K^+$ -production data [20] in order to compare spectra obtained under different kinematical conditions [6,7,20]. The invariant cross section for the  $p+(lN) \rightarrow (lN)+\Lambda+K^+$  reaction is then

$$E \frac{d^3\sigma}{dp^3} \propto \frac{\sqrt{(s_l - m_\Lambda^2 - l^2 m_N^2)^2 - 4m_\Lambda l^2 m_N^2}}{s_l} \quad (2)$$

where  $m_\Lambda$  and  $m_N$  are the  $\Lambda$  and nucleon masses, respectively.  $l$  is the number of nucleons involved in the interaction and

$$s_l = s + m_K^2 - 2E_K(T_p + [l+1]m_N) + 2p_K p_p \cos\theta_K. \quad (3)$$

$m_K$ ,  $E_K$ ,  $p_K$  and  $\theta_K$  are the kaon mass, total energy, momentum and emission angle, respectively, while  $T_p$  and  $p_p$  denote the beam energy and momentum.  $s$  is the square of the CM energy of the incident proton and the  $l$  target nucleons. The solid lines in Fig. 2b) show the momentum dependence of the invariant cross section from Eq. (2) for  $l = 4, 5, 7$ . Although this neglects the intrinsic motion of the  $l$  target nucleons, it shows that kaon production at  $T = 1.0$  GeV can only be understood in terms of cooperative effects with the effective number of nucleons involved in the interaction being  $\sim 5-6$ . It has been suggested [1–5] that such cooperative effects can be described in terms of multi-step mechanisms or high-momentum components in the nuclear wave function.

It has also been pointed out [1–5] that the mechanism of subthreshold  $K^+$  production might be identified from the  $A$ -dependence of the production cross section. The total cross sections measured at PNPI in the energy range  $T = 0.8 - 1.0$  GeV scale as  $\sigma_{\text{tot}} \propto A^1$  [1]. This behavior has been interpreted in terms of a two-step mechanism with the formation of an intermediate  $\pi$ -meson.

We used targets of widely different masses to determine the  $A$ -dependence of the differential cross sections. All measurements were carried out with the same geometry and detection system at ANKE and the same proton beam settings. The ratios of the kaon-production cross sections for various nuclei as a function of kaon momentum  $\sigma_A^{K^+}/\sigma_C^{K^+}$  are therefore equal to the corresponding ratios of kaon count rates in the individual telescopes, normalized to the pion cross-section ratio at a momentum of  $507 \pm 17$  MeV/c detected in telescope #15:

$$\left( \frac{\sigma_A^K}{\sigma_C^K} \right)_{(i)} = \left( \frac{N_A^K}{N_C^K} \right)_{(i)} \frac{M_C^K}{M_A^K} \left( \frac{N_C^\pi}{N_A^\pi} \right)_{(15)} \frac{M_A^\pi}{M_C^\pi} \left( \frac{\sigma_A^\pi}{\sigma_C^\pi} \right)_{(15)}. \quad (4)$$

The cross-section ratios for producing pions with momenta around 500 MeV/c in the forward direction in  $pA$

collisions were measured to better than 10% by several groups in the 0.73–4.2 GeV energy range [17–19,16]. All uncertainties from the efficiency correction  $\epsilon$  in Eq. (1) cancel out for such ratios. The results for Cu/C and Au/C are shown in Fig. 3.

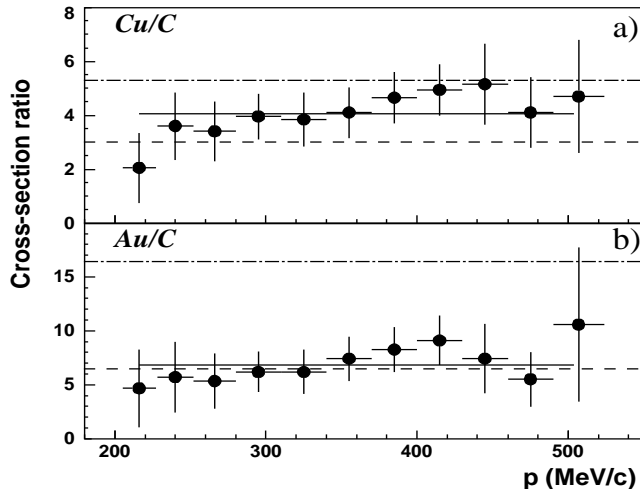


FIG. 3. Ratios of the  $K^+$  production cross sections for Cu/C and Au/C as a function of the kaon momentum. The solid horizontal lines indicate a fit by a constant value. The dashed lines illustrate the ratios if the cross sections scale like  $A^{2/3}$  (dashed) and  $A^1$  (dashed-dotted).

The ratios are almost independent of the  $K^+$ -momentum. The solid lines in Fig. 3 indicate fits with constant values;  $R(\text{Cu}/\text{C}) = 4.0 \pm 0.3$  and  $R(\text{Au}/\text{C}) = 6.8 \pm 0.8$ . These values should be compared to the expected ratios if the cross sections scaled as  $A^1$ :  $R(\text{Cu}/\text{C}) \sim 5$  and  $R(\text{Au}/\text{C}) \sim 16$ . Our data show a significantly weaker  $A$ -dependence with an exponent closer to  $2/3$ . This is in contrast to the behavior of the total cross sections at the same beam energy found in [1], where kaon production was described in terms of the two-step mechanism. It is possible that, due to rescattering of the produced kaons in the target nucleus out of the angular acceptance of ANKE, there is a kaon deficiency at high momenta and small angles. Since this effect should be stronger for heavier targets, it might account for the weaker  $A$ -dependence of the differential cross section.

Summarizing, we have measured small-angle  $K^+$ -production at  $T = 1.0$  GeV, which is far below the free NN threshold. The low-momentum part of the  $K^+$ -spectrum does not follow a thermal distribution whereas the high-momentum part reveals a high collectivity of the target nucleus. Within a simple kinematical model, about 5–6 nucleons are needed to allow kaon production with momenta  $p_K \sim 500$  MeV/c. Alternatively, intrinsic momenta of at least  $p_N \sim 550$  MeV/c are required if such kaons are produced in a collision with a single target nucleon. The target-mass dependence of the differential cross sections shows a scaling significantly weaker than those of the total cross sections [1]. The latter have been

interpreted in terms of two-step  $K^+$ -production. It remains to be shown by microscopic calculations whether this finding is due to rescattering effects of the kaons in the target nucleus or whether it is a reflection of single-step kaon production with high-momentum components in the nuclear wave function.

We would like to acknowledge the assistance we received in performing these measurements at the ANKE spectrometer. Financial support from the following funding agencies was of indispensable help for building ANKE, its detectors and DAQ: Georgia (Department of Science and Technology), Germany (BMBF: grants WTZ-RUS-649-96, WTZ-RUS-666-97, WTZ-RUS-685-99, WTZ-POL-007-99; DFG: 436 RUS 113/337, 436 RUS 113/444, 436 RUS 113/561, State of North-Rhine Westphalia), Poland (Polish State Committee for Scientific Research: 2 P03B 101 19), Russia (Russian Ministry of Science, Russian Academy of Science: 99-02-04034, 99-02-18179a) and European Community (INTAS-98-500).

\* Now working at: Saint-Gobain Crystals & Detectors GmbH, 42929 Wermelskirchen, Germany.

- [1] V.P. Koptev *et al.*, JETP **67**, 2177 (1988).
- [2] W. Cassing *et al.*, Phys. Lett. B **238**, 25 (1990).
- [3] H. Müller and K. Sistemich, Z. Phys. A **344**, 197 (1992)
- [4] A.A. Sibirtsev and M. Büscher, Z. Phys. A **347**, 191 (1994)
- [5] E.Ya. Paryev, Eur. Phys. J. A **5**, 307 (1999).
- [6] S. Schnetzer *et al.*, Phys. Rev. C **40**, 640 (1989).
- [7] M. Debowski *et al.*, Z. Phys. A **356**, 313 (1996).
- [8] A. Badalà *et al.*, Phys. Rev. Lett. **80**, 4863 (1998).
- [9] Yu.T. Kiselev *et al.*, J. Phys. B **25**, 381 (1999).
- [10] J. Julien *et al.*, Phys. Lett. B **264**, 269 (1991).
- [11] P. Senger and H. Ströbele, J. Phys. G **25**, R59 (1999).
- [12] R. Maier, Nucl. Instr. Methods Phys. Res., Sect. A **390**, 1 (1997).
- [13] M. Büscher *et al.*, Phys. Scripta RS **21**, 23 (1993).
- [14] S. Barsov *et al.*, Nucl. Instr. Methods Phys. Res., Sect. A **462/3**, 364 (2001).
- [15] M. Büscher *et al.*, Nucl. Instr. Methods Phys. Res., Sect. A (submitted), available via: <http://ikpd15.ikp.kfa-juelich.de:8085/doc/Publications.html>.
- [16] S. Barsov *et al.*, Acta Phys. Polonica B **31**, 2159 (2000).
- [17] D.R.F. Cochran *et al.*, Phys. Rev. D **6**, 3085 (1972).
- [18] J. Papp *et al.*, Phys. Rev. Lett. **34**, 601 (1975).
- [19] V.V. Abaev *et al.*, J. Phys. G **14**, 903 (1988). **31**, 2159 (2000).
- [20] M. Büscher *et al.*, Z. Phys. A **355**, 93 (1996).
- [21] H. Nifenecker, J.A. Pinston, Prog. Part. Nucl. Phys. **23**, 271 (1989).